NANO LETTERS

2007
Vol. 7, No. 3
825−830

Hidden One-Electron Interactions in Carbon Nanotubes Revealed in Graphene Nanostrips

Carter T. White,*,† Junwen Li,‡ Daniel Gunlycke,† and John W. Mintmire‡

Chemistry Division, Naval Research Laboratory, Washington, DC 20375 and Department of Physics, Oklahoma State University, Stillwater, Oklahoma 74078

Received November 27, 2006; Revised Manuscript Received February 1, 2007

ABSTRACT

Many single-wall carbon nanotube (SWNT) properties near the Fermi level were successfully predicted using a nearest-neighbor tight-binding model characterized by a single parameter, V_1. We show however that this model fails for armchair-edge graphene nanostrips due to interactions directly across hexagons. These same interactions are found largely hidden in the description of SWNTs, where they renormalize V_1 leaving previous nearest-neighbor model SWNT results largely intact while resolving a long-standing puzzle regarding the magnitude of V_1.

Recently, macroscopic single sheets of graphite known as graphene were isolated and found stable, highly crystalline, and chemically inert at ambient conditions.[1] This advance has stimulated increasing interest in graphene nanostrips (GNSs), partly because they could combine the advantages of high-resolution lithography with nanotube-like electronic properties to achieve large-scale integration of ballistic devices.[2] Indeed, the nearest-neighbor tight-binding model, which is successful in describing many of the properties of single-wall carbon nanotube (SWNTs)[3−18], does predict that those strips with armchair edges will have electronic structures very similar to zigzag SWNTs provided their edges are terminated by σ-bonds to H-atoms.[19,20] However, the first-principles results reported below show that the nearest-neighbor approximation fails for these strips in spite of their similarities to SWNTs, even if all C−C bond distances in the strip are assumed identical so that no distortion effects are present. The origin of this failure is traced to the neglect of C−C interactions across hexagons that convert those armchair-edge strips expected to be metallic to semiconductors with gaps that decrease as the inverse widths of the strips. Hence, these interactions should be included explicitly in the description of these strips. However, we also show that these same interactions, although surely present, are largely hidden in the description of SWNTs, leaving previous nearest-neighbor SWNT results intact consistent with the many successes of the nearest-neighbor approximation in predicting the properties of SWNTs.

The armchair-edge GNSs depicted in Figure 1 can be viewed as cut from graphene with their edges terminated by σ-bonds to H-atoms. Each strip can be thought of as series of finite length zigzag chains oriented along the transverse direction of the strip and stacked edge to edge with each zigzag chain containing N carbon atoms. The primitive translational unit cell of the strip contains two such zigzag chains for a total of $2N$ carbon atoms and 4 hydrogen atoms as depicted in Figure 1 for the cases $N = 7$ and $N = 8$. For brevity, we refer to the armchair-edge GNS containing $2N$ carbons in the unit cell as the N armchair-edge GNS. These strips have two different configurations depending on whether N is odd (Figure 1a) or even (Figure 1b). If N is odd, we refer to the strip as symmetric, but if N is even, we refer to it as staggered.

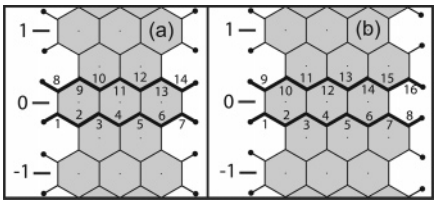

Figure 1. Sample (a) symmetric and (b) staggered armchair edge GNSs with (a) $N = 7$ and (b) $N = 8$. The numbering of the unit cells is shown at the left edge of each figure with only the unit cells labeled 0 shown in their entirety. Each unit cell is composed of two zigzag chains terminated by H atoms with the two chains corresponding to the unit cell labeled 0 shown as darkened. The $2N$ C atoms in a unit cell are numbered as shown.

To study the electronic structure of armchair-edge GNSs, we start by assuming a tight-binding model described by the Hamiltonian, $\hat{H}_0$, which retains only nearest-neighbor π-matrix elements between orthonormal $|p_\pi\rangle$ orbitals (one per carbon atom) oriented normal to the plane of the strip with all diagonal matrix elements fixed at the Fermi level, $\epsilon_F \equiv$

* Corresponding author. E-mail: carter.white@nrl.navy.mil.
† Naval Research Laboratory.
‡ Oklahoma State University.

10.1021/nl0627745 CCC: $37.00
Published on Web 02/13/2007

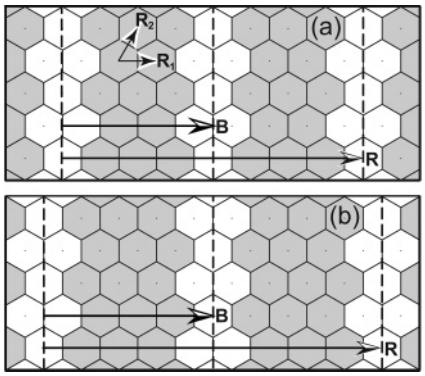

Figure 2. Sample (a) symmetric and (b) staggered N armchair edge GNSs highlighted in gray depicted as embedded in graphene. Two of these strips can also be viewed as embedded in the $(N + 1,0)$ zigzag SWNTs prior to rollup along $\mathbf{R} = (N + 1)\mathbf{R}_1$ so that $\mathbf{R} = 2\mathbf{B}$ with $\mathbf{B}$ the base vector of the GNS.

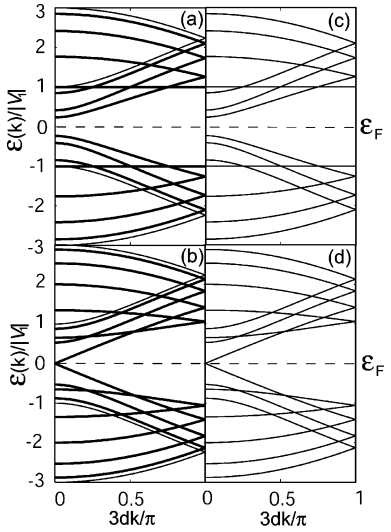

Figure 3. SGSM band structures for the (a) (8,0) and (b) (9,0) SWNTs compared to corresponding (c) 7 and (d) 8 armchair-edge GNSs. Doubly (singly) degenerate bands are shown as thick (thin) lines.

0 eV and all off-diagonal nonzero matrix elements fixed at V_1. This standard graphene sheet model[21] (SGSM) has been used successfully to describe the properties of both graphene and SWNTs near ϵ_F. In addition to including only nearest-neighbor interactions, this model neglects the effects of curvature in SWNTs and assumes all C−C bond lengths, d, and angles are the same in GNSs. The model also assumes that the strip edges are always termimated by compensating dangling sp^2 hybrids at edge C atoms with H atoms to form a strong C−H σ-bonds.[19,20] Nearest-neighbor C−H matrix elements associated with these H-atoms do not appear explicitly in $\hat{H}_0$ because these σ orbitals (like the sp^2 orbitals used to form strong C−C σ bonds in the strip interior) are symmetric with respect to the nodal plane of the π-orbitals and hence decouple from the π-conduction bands described by $\hat{H}_0$. Also, because C forms a strong covalent bond with H, the σ and σ^* bands associated with these bonds lie far from ϵ_F and hence need not be considered further.

Within the SGSM, the band structure of GNSs is contained within the dispersion relations of zigzag SWNTs. To see this, first consider Figure 2 where symmetric and staggered armchair-edge GNSs, are depicted as embedded in graphene. Viewed in this way, we see that if the SGSM is assumed, then the π-band structure of the N armchair-edge strip can be derived from the subset of 2D graphene π-states that vanish at the C atoms along the dashed lines of Figure 2. Formally, this requires that members of this subset have 2D wavevectors, $\mathbf{k}$, such that $\mathbf{k}\cdot\mathbf{B} = \pi m$ where $\mathbf{B}$ is the base vector of the strip depicted in Figure 2 and m is an integer. Furthermore, in applying $\mathbf{k}\cdot\mathbf{B} = \pi m$, only choices for m can be used for which zero coefficients can be generated at the appropriate C atoms; for example $m \neq 0$. Now recall that all SWNT's can be indexed by a pair of integers associated with rolling up a graphene sheet along one of its 2D lattice vectors $\mathbf{R} = n_1\mathbf{R}_1 + n_2\mathbf{R}_2$ to form a (n_1, n_2) cylindrical nanotube[22] with radius r, where $\mathbf{R}_1$ and $\mathbf{R}_2$ are the primitive graphene lattice vectors depicted in Figure 2. Also recall that within the SGSM the band structure of SWNTs defined by $\mathbf{R}$ is obtained from that of graphene by imposing periodic boundary conditions over the rollup vector $\mathbf{R}$ so that $\mathbf{k}\cdot\mathbf{R} = 2\pi m$ with m being an integer.[3−5] However, if $\mathbf{k}\cdot\mathbf{R} = 2\pi m$ for a SWNT with $\mathbf{R} = 2\mathbf{B}$, then $\mathbf{k}\cdot\mathbf{B} = \pi m$ is also satisfied. Thus, within the SGSM, the π-band structure of the N armchair-edge GNS is contained within that of the $(N + 1,0)$ zigzag SWNT which has the rollup vector $\mathbf{R} = 2\mathbf{B}$. Indeed, the band structure of the $(N + 1,0)$ zigzag SWNT and the N armchair-edge GNS are identical within this model except that the four singly degenerate zigzag SWNT bands are missing from the π-band structure of the armchair-edge GNS and the remaining $4N$ doubly degenerate bands of the $(N + 1,0)$ zigzag SWNT become singly degenerate in the N armchair-edge GNS (see Figure 3). The four bands present in the tube, but absent in the strip, lie far from ϵ_F as shown in Figure 3 and need not concern us further. The remaining bands are doubly degenerate in the tube but singly degenerate in the strip because two, rather than one, N armchair-edge GNSs are embedded in the $(N + 1,0)$ zigzag SWNT as illustrated in Figure 2.

Of special interest are the electronic properties of the N armchair-edge strips in the vicinity of ϵ_F, which now can be readily obtained from earlier SWNT results. For example, it is well known that SWNTs are either metallic or semiconducting depending on their structure[3−4,5,10,11] with the $(n_1,0)$ zigzag SWNTs predicted to be metallic by the SGSM if $n_1 = 3q$ with q an integer. This result and the correspondence between the $(N + 1,0)$ SWNT and the N armchair-edge GNS then immediately imply that the N armchair-edge strip will be metallic only if $N + 1 = 3q$, thus recovering the result of Fujita and others obtained by different means.[19,20] It is also known that semiconducting SWNTs with $n_1 - n_2 \neq 3q$ have band gaps given to good approximation by $E_{gap} = |V_1|\, d/r$, if r is the order of the radius of icosahedral C_{60} and greater,[6−8,10,11] where r is the tube radius and d is the C−C bond distance. For the $(N + 1,0)$ zigzag SWNTs, and hence the N armchair-edge strips, this result becomes

$$E_{\text{gap}} = \frac{-2\pi V_1}{\sqrt{3}(N+1)} \quad (1)$$

because $r = \sqrt{3}d(N+1)/2\pi$. Other key expressions can be obtained just as easily from the corresponding SGSM nanotube results[8,13,14] including linear dispersion relations for the metallic strips,[8] the positions of the first few van-Hove singularities in the density of states (DOS) near ϵ_F in both metallic and semiconducting strips,[13] and a universal expression for the DOS near ϵ_F that depends on whether the strip is metallic or semiconducting.[14]

Although eq 1 is known to work well for nanotubes with diameters of the order of C_{60} or larger,[6−11] for the narrower tubes it proves progressively less accurate to the point that it fails completely for the (5,0) SWNT. For the SWNTs, this breakdown occurs because of a combination of factors including curvature induced hybridization,[23,24] direct interactions across the tube,[24] and trigonal warping of the dispersion relations around the *K* points of graphene.[14,25] However, for planar armchair-edge GNSs curvature-induced effects are absent leading to the possibility that eq 1 and related expressions are applicable over a larger range of *N* than found for the corresponding SWNTs. This is consistent with Figure 4, where eq 1 does well even for *N* as small as 4 with deviations now accounted for entirely by trigonal warping. Note though that results such as shown in Figure 4 assume that the one-electron structure of these strips is well described by the SGSM. This assumption is plausible given the success of this model in describing the properties of SWNTs. However, unlike SWNTs where the SGSM was motivated based on first-principles results[3] no similar tests have been made for the armchair-edge strips. Below we present results of such tests that show that this model must be extended to account for the properties of the armchair-edge GNSs, even in the regime where it is known to work well for SWNTs.

Our first-principles results were obtained using an all-electron, self-consistent LCAO local-density functional (LDF) band-structure method originally developed to treat chain polymers.[26] This approach, especially tailored to take advantage of helical symmetry,[27] has been successfully used in wide-ranging studies of SWNTs.[8,14] To obtain the results reported below, we use a 7s3p Gaussian basis for C, a 3s basis for H, and 32 evenly spaced *k* points over the central 1D Brillouin zone in solving the self-consistent LDF equations while assuming that all carbon−carbon (carbon−hydrogen) bond distances are fixed at 0.142 nm (0.108 nm).

LDF results for the band gaps of all armchair-edge GNSs with $4 \le N \le 24$ are presented in Figure 5. Although these results have similarities to the SGSM results of Figure 4, they are also fundamentally different. In particular, although *N* armchair-edge GNSs with $N + 1 = 3q$ have band gaps that are somewhat smaller than similar width strips with $N + 1 \neq 3q$, these gaps are far from zero. The *N* armchair-edge GNSs with $N + 1 = 3q$ should have a gap because they, like the so-called metallic zigzag SWNTs, have an avoided crossing at ϵ_F converting them to semiconductors in the presence of additional interactions.[4,7] However for the $(N + 1,0)$ zigzag SWNTs with $N + 1 = 3q$, this band gap

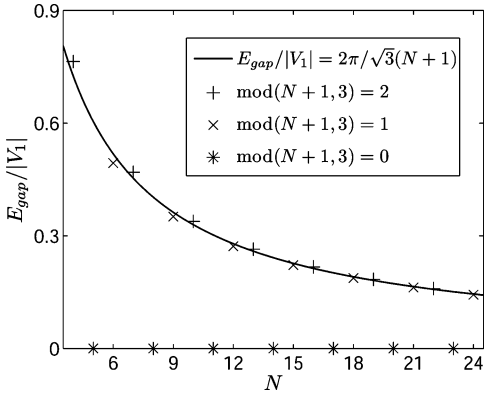

Figure 4. Magnitude of HOMO−LUMO gap of the *N* armchair-edge GNSs from the SGSM.

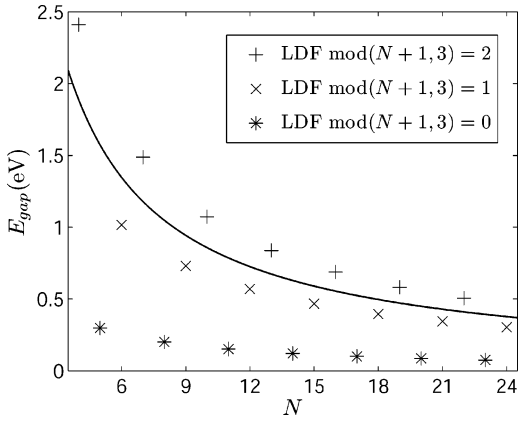

Figure 5. Magnitude of the HOMO−LUMO gap of the *N* armchair-edge GNSs from the LDF calculations. Also shown as a solid line are results from eq 1 of the text for the semiconducting strips, $\mathrm{mod}(N + 1,3) \neq 0$, assuming $V_1 = -2.6$ eV.

scales as $1/(N+1)^2$ (refs 28−30) leading to a correction far smaller than what is seen in Figure 5 for the corresponding GNSs. Also, the gap in the quasi-metallic zigzag SWNTs arises principally from the effects of curvature, which are absent in the GNSs. Hence, the GNS gap at ϵ_F would be expected to be smaller not larger than the corresponding SWNT gap. In addition, although the armchair-edge strips with $N + 1 \neq 3q$ are semiconductors as predicted by the SGSM, this same model requires that these strips have semiconducting gaps that decrease monotonically with increasing strip width (see Figure 4). However, Figure 5 shows that the $N = 3q$ strips have significantly smaller semiconducting gaps than those with $N = 3q + 1$. Therefore, in dealing with armchair-edge GNSs the SGSM must be modified. Furthermore, in making these modifications we do not appeal to distortion effects because in our first-principles results all C−C bonds are assumed equal.

Hydrogen atoms at the strip edges are one possible source of modifications to $\hat{H}_0$. Thus far we have assumed that these atoms compensate the C dangling σ-bonds without otherwise affecting the electronic structure near ϵ_F. However, these edge hydrogens will also produce a small shift in the potential at the edge carbons. These interactions can be incorporated into the model by adding a term $\hat{U}_{\text{edge}}$ to $\hat{H}_0$ that shifts the site diagonal terms of $\hat{H}_0$ at the edge carbons by ϵ_{edge}. Longer-

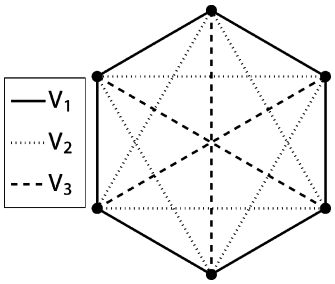

Figure 6. Depiction of various interactions between C atoms treated in the text.

range interactions between C atoms[31] such as depicted in Figure 6 provide another source of potentially important modifications as they allow direct coupling between C atoms across the dashed lines of Figure 2 so that the band structure of the N armchair-edge GNS is no longer embedded in that of the $(N + 1,0)$ SWNT. These longer-range interactions can be incorporated into the model by adding $\hat{U}_{V_2}$ and $\hat{U}_{V_3}$ to $\hat{H}_0$, where $\hat{U}_{V_2}$ ($\hat{U}_{V_3}$) includes all next-nearest-neighbor (next−next-nearest-neighbor) interactions V_2 (V_3) between C atoms in the armchair-edge GNS. Even longer range interactions could also be included but they are expected to fall off quickly with distance and ultimately prove unnecessary.

Because $|\epsilon_{\text{edge}}/V_1|$, $|V_2/V_1|$, and $|V_3/V_1|$ are small, $\hat{U} = \hat{U}_{\text{edge}} + \hat{U}_{V_2} + \hat{U}_{V_3}$ can be treated as a perturbation to $\hat{H}_0$. Also, because $\hat{U}$ does not break the translation symmetry of the strip, it couples only states with the same k. In addition, the armchair-edge strips are direct band gap materials with the HOMO and LUMO states occurring at $k = 0$ (see Figure 3). Therefore, we need only to consider the eigenstates of $\hat{H}_0$ at $k = 0$ in evaluating the effects of $\hat{U}$ on the magnitude of the HOMO−LUMO gap, E_{gap}. Moreover, at $k = 0$ the eigenstates of $\hat{H}_0$ for the N armchair-edge GNS are given by

$$|\Psi_p^{\pm}\rangle = \frac{1}{\sqrt{N_{\text{cell}}}}\frac{1}{\sqrt{N+1}}\sum_l\sum_{n=1}^{N}\left[\sin\left(\frac{pn\pi}{N+1}\right)\right](|n, l\rangle \pm |n+N, l\rangle) \quad (2)$$

where $1 \le p \le N$, and $|n, l\rangle$ denotes the $|p_\pi\rangle$ orbital associated with the nth C atom in the unit cell labeled by l in the notation of Figure 1. Combining this result with the above observations, we then find in the presence of V_1, V_2, V_3, and ϵ_{edge} that E_{gap} is given to lowest order in perturbation theory by

$$E_{\text{gap}} = 2V_1\left[2\cos\left(\frac{p\pi}{N+1}\right) + s\right] + s\frac{2V_3}{N+1}\left[3 + N + 2(N-1)\cos\left(\frac{2p\pi}{N+1}\right) + 2\cos\left(\frac{2p\pi N}{N+1}\right)\right] \quad (3)$$

where: if $\text{mod}(N + 1,3) = 0$, then $p = (N + 1)/3$ and $s = -1$; if $\text{mod}(N + 1,3) = 1$, then $p = (2N + 3)/3$, and $s = 1$; and, if $\text{mod}(N + 1,3) = 2$, then $p = (N + 2)/3$, and $s = -1$. The first term on the right-hand side of eq 3 is the gap due to $\hat{H}_0$; when $N + 1$ is large and $N + 1 \neq 3q$ this term reduces to the right-hand side of eq 1. The second term gives the lowest order correction due to $\hat{U}$. Although $\hat{U}_{\text{edge}}$ and $\hat{U}_{V_2}$ both contribute to $\hat{U}$, neither ϵ_{edge} nor V_2 appears in eq 3 because to first order they shift the HOMO and LUMO levels by the same amount: $3(\epsilon_{\text{edge}} - NV_2)/(N + 1)$. If $N + 1 = 3q$ and $\hat{U}_{V_3} = 0$, then $\hat{U}_{\text{edge}} + \hat{U}_{V_2}$ will open a gap at ϵ_F but for reasonable choices of ϵ_{edge} and V_2 these higher order corrections are far too small to explain the gap observed in the LDF results.

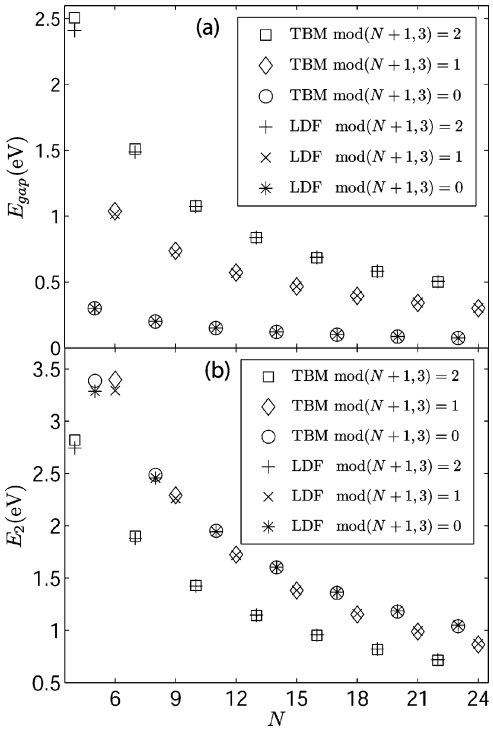

Figure 7. LDF results for (a) E_{gap} and (b) E_2 compared to the corresponding tight-binding model (TBM) results obtained from eq 3 with $V_1 = -3.2$ eV and $V_3 = -0.3$ eV.

If $N + 1 = 3q$, the first term on the right-hand side of eq 3 vanishes leaving only the second term which reduces to

$$E_{gap} = -\frac{6V_3}{N+1} \quad (4)$$

Therefore, eq 4 can be used to least-squares fit the LDF data for $N + 1 = 3q$ to determine V_3 and then with V_3 fixed at this value V_1 can be determined by using eq 3 to least-squares fit the LDF data for $N + 1 \neq 3q$. Implementing this procedure yields the physically reasonable results: $V_1 = -3.2$ eV and $V_3 = -0.3$ eV, which provide an excellent fit to the LDF results for all N as shown in Figure 7a. Furthermore, for the same parameters the right-hand side of eq 3 yields the separation, E_2, between the next to lowest unoccupied state and next to the highest occupied state at $k = 0$, which also is in excellent agreement with the corresponding LDF results as shown in Figure 7b. (Note that in obtaining E_2 from eq 3, p and s are chosen to correspond to the next to lowest unoccupied state, which implies that if $\text{mod}(N + 1,3) = 0$, then $p = (2N + 5)/3$ and $s = 1$; if $\text{mod}(N + 1,3) = 1$,

then $p = (N + 3)/3$, and $s = -1$; and, if mod$(N + 1,3) = 2$, then $p = 2(N + 2)/3$, and $s = 1$.) Other useful results can be also obtained from eq 3 such as the behavior of E_{gap} when $N + 1 \neq 3q$ and N is large

$$E_{\text{gap}} = -\frac{2\pi(V_1 - 2V_3)}{\sqrt{3}(N+1)} \pm \frac{6V_3}{N+1} \tag{5}$$

where if mod$(N + 1,3) = 1$ [mod$(N + 1,3) = 2$], then the plus [minus] sign applies.

The results so far imply that the SGSM should be extended to include C−C interactions directly across hexagons to reproduce the LDF results for armchair-edge GNSs near ϵ_F. This is puzzling because these interactions, although present and of similar strength, have proven unnecessary in describing the one-electron properties of SWNTs in the same region.[3−18] To address this conundrum, consider the tight-binding dispersion relations of graphene in the presence of V_1, V_2, and V_3:

$$\epsilon_{\pm}(\mathbf{k}) = V_2 A(\mathbf{k}) \pm \sqrt{V_1^2[3 + A(\mathbf{k})] + 2V_1V_3B(\mathbf{k}) + V_3^2C(\mathbf{k})} \tag{6}$$

where

$$A(\mathbf{k}) = 2[\cos\mathbf{k}\cdot\mathbf{R_1} + \cos\mathbf{k}\cdot\mathbf{R_2} + \cos\mathbf{k}(\mathbf{R_1} - \mathbf{R_2})] \tag{7}$$

$$B(\mathbf{k}) = [1 + 2\cos\mathbf{k}\cdot(\mathbf{R_1} - \mathbf{R_2})][1 + \cos\mathbf{k}\cdot\mathbf{R_1} + \cos\mathbf{k}\cdot\mathbf{R_2}] + \cos\mathbf{k}\cdot(\mathbf{R_1} + \mathbf{R_2}) - 1 \tag{8}$$

$$C(\mathbf{k}) = 8\cos\mathbf{k}\cdot\mathbf{R_1}\cos\mathbf{k}\cdot\mathbf{R_2}\cos\mathbf{k}\cdot(\mathbf{R_1} - \mathbf{R_2}) + 1 \tag{9}$$

and $\mathbf{k}$ is restricted to the usual hexagonal unit cell (central Brillouin zone) of the graphene reciprocal lattice with primitive reciprocal lattice vectors $\mathbf{K_1}$ and $\mathbf{K_2}$ defined by $\mathbf{K}_i\cdot\mathbf{R}_j = 2\pi\delta_{ij}$. Of special interest are states with wavevectors in the vicinity of the two inequivalent corners (K points) of the central Brillouin zone located at $\mathbf{k}_F \equiv (\mathbf{K}_1 - \mathbf{K}_2)/3$ and $(2\mathbf{K}_1 + \mathbf{K}_2)/3$, because states with these $\mathbf{k}$ lie near ϵ_F. Although $\epsilon_{\pm}(\mathbf{k})$ has cusps at $\mathbf{k}_F$, $[\epsilon_{\pm}(\mathbf{k}) - V_1A(\mathbf{k})]^2$ is well behaved and can be expanded in a Taylor series in terms of $\Delta k \equiv a|\mathbf{k} - \mathbf{k}_F|$ to get

$$\epsilon_{\pm}(\mathbf{k}) = -3V_2 \pm \frac{\sqrt{3}}{2}|V_1 - 2V_3|a|\mathbf{k} - \mathbf{k}_F| \tag{10}$$

valid to first order in $a|\mathbf{k} - \mathbf{k}_F|$ with $a = \sqrt{3}d$. If the effects of curvature are neglected, analytic results for the band gaps,[6] dispersion relations,[8] positions of the van-Hove singularities,[13] and DOS[14] of SWNTs near ϵ_F can be derived from eq 10 by applying periodic boundary conditions over the SWNT rollup vector $\mathbf{R}$. The only differences between eq 10 and the corresponding expression from the SGSM with $V_2 = V_3 = 0$ eV is an unimportant constant that arises from V_2 and a different interpretation of the slope of $\epsilon_{\pm}(\mathbf{k})$ in terms of the underlying parameters V_1 and V_3. Therefore, in the presence of V_2 and V_3 the analytic forms of the earlier SWNT results, which rest on a single parameter determined by the slope the linear dispersion relations of graphene, remain intact; it is only the interpretation of V_{eff} that enters these expressions that has changed. For example, Figure 8 shows that eq 1 remains a good approximation to the HOMO−LUMO separation in zigzag SWNTs in the presence of V_2 and V_3, provided V_1 is replaced by $V_{\text{eff}} = V_1 - 2V_3$. Furthermore, in earlier studies it was the slope $\sqrt{3}aV_{\text{eff}}/2$, not the underlying parameters, that was fit to the first-principles SWNT results[3,8,9,14] and experiment[10,11,15−17] to extract a value of V_{eff}. However, this way of determining V_{eff} automatically includes the effects of both V_1 and V_3. Therefore, V_2 and V_3 are largely hidden in describing the electronic properties of SWNTs near ϵ_F. Nevertheless, V_3 remains important to the understanding of SWNTs; for example, it explains why $|V_{\text{eff}}|$ for these tubes is smaller than $|V_{\text{eff}}|$ for the prototypical electroactive polymer all-trans polyacetylene, $(CH)_x$, thus resolving a long-standing issue regarding the relatively small size of V_{eff} in SWNTs.[3] In particular, owing to the geometry of all-trans $(CH)_x$, V_3 is not present so that $V_{\text{eff}} \approx V_1$, but in the SWNTs V_3 is present and reduces the bare nearest-neighbor C−C coupling to an effective value, $V_{\text{eff}} \approx V_1 - 2V_3$, consistent both with results of STM experiments[10,11,16,17] and first-principles calculations[3,8,9,14] on SWNTs (−2.5 to −2.6 eV).

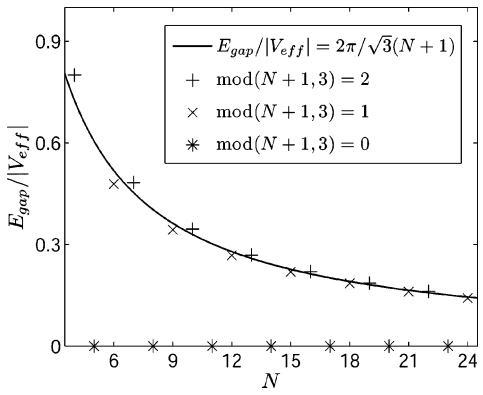

Figure 8. Magnitude of HOMO−LUMO gap of the $(N + 1,0)$ zigzag SWNT from the TBM with $V_1 = -3.2$ eV, $V_2 = -0.5$ eV, and $V_3 = -0.3$ eV compared to results from eq 1 of the text with V_1 replaced by $V_{\text{eff}} = V_1 - 2V_3$. The tight-binding results are practically indistinguishable from those obtained from the SGSM with $V_1 = -2.6$ eV (see Figure 4). Note that $V_2 = -0.5$ eV is assumed for illustrative purposes only and could just as well be taken with opposite sign; to first order in $|V_2/V_1|$, V_2 has no effect on Figures 7 and 8. Also note that these results neglect curvature effects, which become important for nanotubes with radii less than the (10,0).

Our results demonstrate that although many of the properties of SWNTs near ϵ_F are well treated within the SGSM, this same model can fail in this region for other closely related carbon nanostructures such as armchair-edge GNSs due to the neglect of C−C interactions directly across hexagons. As such, these results have consequences not only in the modeling for GNSs but also for many other related carbon-based nanostuctures and polymers. These longer-range one-electron interactions should certainly be considered before incorporating more complex effects such as those arising from electron−lattice and electron−electron interac-

tions described by many-body Hamiltonians. Whether or not they are important will depend on the system. For example, unlike the armchair-edge GNSs, we find that it makes little difference whether these interactions are included explicitly or simply absorbed into an effective nearest-neighbor coupling in the tight-binding band structure of zigzag-edge GNSs.

Finally, after this paper was completed we became aware of two other first-principles studies that also find that the armchair-edge GNSs can be divided into three semiconducting families depending on their widths.[32,33] Neither work however identifies interactions directly across hexagons, a principal focus of this paper, as important in explaining this behavior.

Acknowledgment. This work was supported by ONR both directly and through the Naval Research Laboratory.

References

(1) Novoselov, K. S.; Jiang, D.; Schedin, F.; Booth, T. J.; Khotkevich, V. V.; Morozov, S. V.; Geim, A. K. *Proc. Natl. Acad. Sci. U.S.A.* **2005**, *102*, 10451.
(2) Berger, C.; Song, Z.; Li, T.; Li, X.; Ogbazghi, A. Y.; Feng, R.; Dai, Z.; Marchenkov, A. N.; Conrad, E. H.; First, P. N.; de Heer, W. A. *J. Phys. Chem. B* **2004**, *108*, 19912.
(3) Mintmire, J. W.; Dunlap, B. I.; White, C. T. *Phys. Rev. Lett.* **1992**, *68*, 631.
(4) Hamada, N.; Sawada, S.; Oshiyama, A. *Phys. Rev. Lett.* **1992**, *68*, 1579.
(5) Saito, R.; Fujita, M.; Dresselhaus, G.; Dresselhaus, M. S. *Appl. Phys. Lett.* **1992**, *60*, 2204.
(6) White, C. T.; Robertson, D. H.; Mintmire, J. W. *Phys. Rev B* **1993**, *47*, 5485.
(7) White, C. T.; Mintmire, J. W.; Mowrey, R. C.; Brenner, D. W.; Robertson, D. H.; Harrison, J. A.; Dunlap, B. I. In *Buckminsterfullerenes*; Billups, W. E., Ciufolini, M. A., Eds.; VHS Publishers, Inc.: New York, 1993; p 125.
(8) Mintmire, J. W.; Robertson, D. H.; White, C. T. *J. Phys. Chem. Solids* **1993**, *54*, 1835.
(9) Mintmire, J. W.; White, C. T. *Carbon* **1995**, *33*, 893.
(10) Wildöer, J. W. G.; Venema, L. C.; Rinzler, A. G.; Smalley, R. E.; Dekker, C. *Nature* **1998**, *391*, 59.
(11) Odom, T. W.; Huang, J.-L.; Kim, P.; Lieber, C. M. *Nature* **1998**, *391*, 62.
(12) Mintmire, J. W.; White, C. T. *Appl. Phys. A* **1998**, *67*, 65.
(13) White, C. T.; Mintmire, J. W. *Nature* **1998**, *394*, 29.
(14) Mintmire, J. W.; White, C. T. *Phys. Rev. Lett.* **1998**, *81*, 2506.
(15) Tang, X.-P.; Kleinhammes, A.; Shimoda, H.; Fleming, L.; Bennoune, K. Y.; Sinha, S.; Bower, C.; Zhou, O.; Wu, Y. *Science* **2000**, *288*, 492.
(16) Lemay, S. G.; Janssen, J. W.; van den Hout, M.; Mooij, M.; Bronikowski, M. J.; Willis, P. A.; Smalley, R. E.; Kouwenhoven, L. P.; Dekker, C. *Nature* **2001**, *412*, 617.
(17) Ouyang, M.; Huang, J. L.; Lieber, C. M. *Phys. Rev. Lett.* **2002**, *88*, 066804.
(18) White, C. T.; Mintmire, J. W. *J. Phys. Chem. B* **2005**, *109*, 52.
(19) Fujita, M.; Wakabayashi, K.; Nakada, K.; Kusakabe, K. *J. Phys. Soc. Jpn.* **1996**, *65*, 1920.
(20) Nakada, K.; Fujita, M.; Dresselhaus, G.; Dresselhaus, M. S. *Phys. Rev. B* **1996**, *54*, 17954.
(21) Wallace, P. R. *Phys. Rev.* **1947**, *71*, 622.
(22) Iijima, S.; Ichihashi, T. *Nature* **1993**, *363*, 603.
(23) Blase, X.; Benedict, L. X.; Shirley, E. L.; Louie, S. G. *Phys. Rev. Lett.* **1994**, *72*, 1878.
(24) Cabria, I.; Mintmire, J. W.; White, C. T. *Phys. Rev. B* **2003**, *67*, 121406.
(25) Saito, R.; Dresselhaus, G.; Dresselhaus, M. S. *Phys. Rev. B* **2000**, *61*, 2981.
(26) Mintmire, J. W.; White, C. T. *Phys. Rev. Lett.* **1983**, *50*, 101.
(27) Mintmire, J. W. In *Density Functional Methods in Chemistry*; Labanowski, J. K., Andzelm, J. W., Eds.; Springer-Verlag, New York, 1991; p 125.
(28) White, C. T.; Robertson, D. H.; Mintmire, J. W. In *Clusters and Nanostructured Materials*; Jena, P., Behera, S. N., Eds.; Nova Science Publishers, Inc.: New York, 1996; p 231.
(29) Kane, C. L.; Mele, E. J. *Phys. Rev. Lett.* **1997**, *78*, 1932.
(30) Ouyang, M.; Huang, J.-L.; Cheung, C. L.; Lieber, C. M. *Science* **2001**, *292*, 702.
(31) Reich, S.; Maultzsch, J.; Thomsen, C.; Ordejón, P. *Phys. Rev. B* **2002**, *66*, 035412.
(32) Son, Y.-W.; Cohen, M. L.; Louie, S. G. *Phys. Rev. Lett.* **2006**, *97*, 216803.
(33) Barone, V.; Hod, O.; Scuseria, G. E. *Nano Lett.* **2006**, *6*, 2748.

NL0627745